Refereed Proceedings

The 12th International Conference on Fluidization - New Horizons in Fluidization Engineering

Engineering Conferences International *Year* 2007

Time Scale Analysis of a Fluidized-Bed Catalytic Reactor Based on a Generalized Dynamic Model

Andres Mahecha-Botero* John R. Grace†
Said S.E.H. Elnashaie‡ C. Jim Lim**

*University of British Columbia, andresm@chml.ubc.ca
†University of British Columbia, jgrace@chml.ubc.ca
‡Pennsylvania State University, nashaie@chml.ubc.ca
**The University of British Columbia, cjlim@chml.ubc.ca

TIME-SCALE ANALYSIS OF A FLUIDIZED-BED CATALYTIC REACTOR BASED ON A GENERALIZED DYNAMIC MODEL

Andrés Mahecha-Botero, John R. Grace, Said S.E.H. Elnashaie, C. Jim Lim
Department of Chemical and Biological Engineering, University of British Columbia, 2360 East Mall, Vancouver, Canada. V6T1Z3.
T: 1-604-822-3457; F: 1-604-822-6003; E: andresm@chml.ubc.ca

ABSTRACT

A fluidized-bed reactor model is implemented to simulate a Maleic Anhydride (MA) reactor with special emphasis on its dynamic behaviour. The dynamic model is general enough that it can treat a wide range of catalytic systems, subject to mass and energy balances within the phases. The model represents multiple phases and regions (low-density phase, high-density phase, freeboard region) and can account for heat and mass axial and radial anisotropic dispersion, change in molar/volumetric flow due to reaction, temperature and pressure profiles, hydrodynamic regime variation, catalyst deactivation, energy options, and multiple membranes of various geometries for introduction/extraction of any compound. The model reduces, as special cases, to most fluidized bed reactor models reported in the literature, allowing the influence of simplifying assumptions to be investigated. Introduction of different assumptions for a MA fluidized-bed reactor of industrial scale reveal quite different predicted time scales for key dynamic phenomena inherent to the process. A mass transfer/reaction time scale was found to be close to the residence time of the gas molecules in the reactor. The heat transfer time scale is several orders of magnitude larger for the current system. This type of time-scale analysis may be a useful tool to identify the appropriate degree of sophistication to predict the dynamics of complex reacting systems.

INTRODUCTION

Fluidized-bed reactors, like many other industrial and natural processes, involve multiple phenomena that occur at different rates. In a fluidized-bed reactor, phenomena such as multi-phase flow, mass transfer/reaction and heat transfer take place in coupled non-linear ways. Dynamic modelling for such phenomena requires mathematical relations that describe the interaction between the system state variables and parameters, accounting for their evolution in time. In this paper, a comprehensive dynamic model is presented, and its different time scales are identified to gain insight into the dynamic behaviour of fluidized-beds.

Predicting the behaviour of gas-solid fluidized-bed reactors requires information on reaction kinetics, stoichiometry, thermodynamics, heat and mass transfer and flow patterns of the different phases in the reactor. Many reactor models have been proposed in the literature. In addition to those reviewed by Yates (1), Grace (2) and Ho (3), more recent ones include Thompson *et al.* (4), Abba *et al.* (5) and Chen *et al.* (6). Each of these incorporates a different set of assumptions, leading to a different set of mathematical expressions to simulate the reactor. This paper uses a comprehensive model that builds upon most of the features from previous modelling efforts, including dynamic behaviour.

The dynamic behaviour of complex systems often contains multiple time scales (7). After an initial transient period, it may be possible to consider some fast phenomena as if they were instantaneous relative to slower ones (7). For instance, hydrodynamic phenomena may reach a pseudo-steady state much more quickly than heat transfer in fluidized bed reactors. The

identification of different time scales may then be used to simplify the numerical solution of the system model (8-11).

The 12th International Conference on Fluidization - New Horizons in Fluidization Engineering, Art. 76 [2007]

FUNDAMENTAL DIFFERENTIAL DYNAMIC MODEL FOR CATALYTIC SYSTEMS

A generalized dynamic model is developed for gas-solid catalytic fluidized-bed reactors. For further details regarding this model see Mahecha-Botero et al. (12-14).

Mole Balance

The molar rate balance over a differential element for phase *(φ)* is given by:

[Convective input – Convective output]$_{(gas+cat+seq)}$ + [Diffusive input – Diffusive output] $_{(gas)}$ + [Reaction generation/consumption] $_{(cat+seq)}$ + [Exchange] $_{(\varphi)}$ = [Accumulation rate] $_{(gas+cat+seq)}$

The number of mole balance equations is $N_C.N_{(\varphi)}$. The terms in the general mole balance for component *i* in phase *(φ)* are shown in symbols as follows:

$$
\begin{aligned}
&-\varepsilon_{(\varphi)}.\left\{\vec{\nabla}.\left[C_{i_{(\varphi)}}.\overrightarrow{U_{gas_{(\varphi)}}}\right]\right\}-\left(1-\varepsilon_{(\varphi)}\right).\left\{\left(1-\alpha_{(\varphi)}\right).\vec{\nabla}.\left[f_C\left(C_{i_{(\varphi)}}\right).\overrightarrow{U_{cat_{(\varphi)}}}\right]+\alpha_{(\varphi)}.\vec{\nabla}.\left[f_S\left(C_{i_{(\varphi)}}\right).\overrightarrow{U_{seq_{(\varphi)}}}\right]\right\}\\
&-\varepsilon_{(\varphi)}.\vec{\nabla}.(\overrightarrow{N_{i_{(\varphi)}}})+\left(1-\varepsilon_{(\varphi)}\right).\left\{\left(1-\alpha_{(\varphi)}\right).\rho_{cat}.\sum_{j=1}^{N_{Rcat}}\sigma_{ij_{cat(\varphi)}}.\eta_{j_{cat(\varphi)}}.\chi_{j_{cat(\varphi)}}.r_{j_{cat(\varphi)}}\right\}\\
&+\left(1-\varepsilon_{(\varphi)}\right).\left\{\alpha_{(\varphi)}.\rho_{seq}.\sum_{j=1}^{N_{Rseq}}\sigma_{ij_{seq(\varphi)}}.\eta_{j_{seq(\varphi)}}.\chi_{j_{seq(\varphi)}}.r_{j_{seq(\varphi)}}\right\}=\varepsilon_{(\varphi)}.\frac{\partial C_{i_{(\varphi)}}}{\partial t}\\
&+\left(1-\varepsilon_{(\varphi)}\right).\left(1-\alpha_{(\varphi)}\right).S_{cat_{(\varphi)}}.\frac{\partial\left[f_C\left(C_{i_{(\varphi)}}\right)\right]}{\partial t}+\left(1-\varepsilon_{(\varphi)}\right).\alpha_{(\varphi)}.S_{seq_{(\varphi)}}.\frac{\partial\left[f_S\left(C_{i_{(\varphi)}}\right)\right]}{\partial t}.
\end{aligned}
\tag{1}
$$

Here $C_{i_{(\varphi)}}$ is the concentration of species *i*, $\overrightarrow{U_{(\varphi)}}$ the vector of convective velocity, $\overrightarrow{N_{i(\varphi)}}$ the vector of dispersive molar fluxes (calculated using Fick's or Stefan-Maxwell diffusion).

Energy Balance

The differential energy balance for phase *(φ)* is given by:

[Convective heat input – Convective heat output]$_{(gas+cat+seq)}$ + [Diffusive heat input – Diffusive heat output] $_{(gas)}$ + [Chemical reaction heat generation/consumption] $_{(cat+seq)}$ + [Heat exchange with other phases and surroundings] $_{(\varphi)}$ = [Heat accumulation rate] $_{(gas+cat+seq)}$

$$
\begin{aligned}
&-\varepsilon_{(\varphi)}.\left\{\vec{\nabla}.\left[\left(\sum_{i=1}^{NC}C_{i_{(\varphi)}}.E_{i_{(\varphi)}}\right).\overrightarrow{U_{gas_{(p)}}}\right]\right\}-\left(1-\varepsilon_{(\varphi)}\right).\left(1-\alpha_{(\varphi)}\right).\vec{\nabla}.\left[\left(S_{cat_{(\varphi)}}.\sum_{i=1}^{NC}f_C\left(C_{i_{(\varphi)}}\right).E_{i_{cat(\varphi)}}+\rho_{cat}.E_{cat_{(\varphi)}}\right).\overrightarrow{U_{cat_{(\varphi)}}}\right]\\
&-\left(1-\varepsilon_{(\varphi)}\right).\alpha_{(\varphi)}.\vec{\nabla}.\left[\left(S_{seq_{(\varphi)}}.\sum_{i=1}^{NC}f_S\left(C_{i_{(\varphi)}}\right).E_{i_{seq(\varphi)}}+\rho_{seq}.E_{seq_{(\varphi)}}\right).\overrightarrow{U_{seq_{(\varphi)}}}\right]-\vec{\nabla}.(\overrightarrow{q_{(\varphi)}})\\
&+\left(1-\varepsilon_{(\varphi)}\right).\left\{\left(1-\alpha_{(\varphi)}\right).\rho_{cat}.\sum_{j=1}^{N_{Rcat}}\Delta H_{j_{cat}}.\eta_{j_{cat(\varphi)}}.\chi_{j_{cat(\varphi)}}.r_{j_{cat(\varphi)}}+\alpha_{(\varphi)}.\rho_{seq}.\sum_{j=1}^{N_{Rseq}}\Delta H_{j_{seq}}.\eta_{j_{seq(\varphi)}}.\chi_{j_{seq(\varphi)}}.r_{j_{seq(\varphi)}}\right\}\\
&=\varepsilon_{(\varphi)}.\frac{\partial}{\partial t}\sum_{i=1}^{NC}C_{i_{(\varphi)}}.E_{i_{(\varphi)}}+\left(1-\varepsilon_{(\varphi)}\right).\left(1-\alpha_{(\varphi)}\right).\frac{\partial}{\partial t}\left(S_{cat_{(\varphi)}}.\sum_{i=1}^{NC}f_C\left(C_{i_{(\varphi)}}\right).E_{i_{cat(\varphi)}}+\rho_{cat}.E_{cat_{(\varphi)}}\right)\\
&+\left(1-\varepsilon_{(\varphi)}\right).\alpha_{(\varphi)}.\frac{\partial}{\partial t}\left(S_{seq_{(\varphi)}}.\sum_{i=1}^{NC}f_S\left(C_{i_{(\varphi)}}\right).E_{i_{seq(\varphi)}}+\rho_{seq}.E_{seq_{(\varphi)}}\right).
\end{aligned}
\tag{2}
$$

The terms in the general balance are shown in symbols above. The number of energy

balance equations is $M_{(\varphi)}$. Here $E_{i_{(\varphi)}}$ is the internal energy of component *i*, and $\overrightarrow{q_{(\varphi)}}$ is the vector of conductive heat fluxes (calculated using Fourier's law of conduction). Other symbols in these conservation equations are defined in the Notation section.

Pressure Balance

A simplified differential pressure balance in the z-direction for phase *(φ)* is given by:

$$-\frac{dP_{(\varphi)}}{dz} = \left\{(1-\varepsilon_{(\varphi)}).\left[(1-\alpha_{(\varphi)})\rho_{cat} + \alpha_{(\varphi)}.\rho_{seq}\right] + \varepsilon_{(\varphi)}.\rho_{gas}\right\}g. \quad \textbf{(3)}$$

Boundary and Initial Conditions

The boundary conditions may assume axial symmetry, zero flux at the walls and Danckwerts criteria (15) with diffusion assumed to be negligible in the fore and after sections. A base set of boundary conditions is displayed in Table 1.

Table 1. Boundary and initial conditions.

At $z=0$: $-K_z.\frac{\partial T_{(\varphi)}}{\partial z} = U_{gas_{(\varphi)}}.A.\rho_{(\varphi)}.\left\langle C_{p_{(\varphi)}}\right\rangle.\left(T_{(\varphi)}\right]_{0^-} - T_{(\varphi)}\left]_{0^+}\right)$, $-D_{i(\varphi)_z}.\frac{\partial C_{i_{(\varphi)}}}{\partial z} = U_{gas_{(\varphi)}}.\left(C_{i_{(\varphi)}}\right]_{0^-} - C_{i_{(\varphi)}}\left]_{0^+}\right)$, $P_{(\varphi)} = \left(P_{(\varphi)}\right)_{(z=0)}$.	
At $z=L$: $\frac{\partial C_{i_{(\varphi)}}}{\partial z}=0$, $\frac{\partial T_{(\varphi)}}{\partial z}=0$.	At $t=0$: $C_{i_{(\varphi)}} = \left(C_{i_{(\varphi)}}\right)_{t=0}$, $T_{(\varphi)} = \left(T_{(\varphi)}\right)_{t=0}$.

CASE STUDY: APPLICATION TO AN INDUSTRIAL MA FLUIDIZED-BED REACTOR

Maleic Anhydride (MA) is an important intermediate in the production of fumaric and tartaric acids, unsaturated polyester resins, chemicals for agriculture, alkid resins, lubricant oils, copolymers, food additives and NutraSweet (16, 17). Initially, MA was produced from benzene (17), but due to environmental and economic constraints, it is currently produced commercially by partial oxidation of n-butane over a vanadium phosphorous oxide(VPO) catalyst (18), involving complex heterogeneously-catalyzed reactions (19) and the only alkane-selective oxidation reaction used in industry (20). The catalytic reactions occur through sequential reduction-oxidation of the catalyst surface and selective generation of MA (21). Fluidized bed reactors now play a major role in MA synthesis, facilitating excellent heat transfer and avoiding hot spots. As well, higher reactant concentrations can be fed without generating explosive mixtures because the fluidized catalyst acts as a flame arrester (22). The dimensions and operating conditions given in Table 2, are similar to those in some industrial units.

Reaction Kinetics (23)

The well-documented kinetics of Centi *et al.* (23) were employed in our simulations. These are widely used (17, 24) and can produce accurate species conversion predictions (25). A triangular reaction scheme commonly appears in the literature (17, 24, 25), based on the earlier work of Centi et al. (23). The reaction rates are then described by:

$$r_1 = r_{C_4H_2O_3} = \frac{k_1 C_{C_4H_{10}} C_{O_2}{}^{\alpha}}{1+K_B C_{C_4H_{10}}}; \quad \textbf{(4)} \qquad r_2 = r_{CO_x} = k_2 C_{O_2}^{\beta}; \quad \textbf{(5)} \qquad r_3 = k_3 C_{C_4H_2O_3}\left(\frac{C_{O_2}^{\gamma}}{C_{C_4H_{10}}^{\delta}}\right). \quad \textbf{(6)}$$

where r_1 is the rate of MA formation, r_2 the rate of butane total oxidation, and r_3 the rate of MA

total oxidation. The corresponding kinetic constants (23) appear in Table 3.

The 12th International Conference on Fluidization - New Horizons in Fluidization Engineering, Art. 76 [2007]

Table 2. Key reactor parameters

Parameter	Value	Parameter	Value
Gas inlet temperature	613 [K]	Catalyst density	2000 [kg/m^3]
Pressure at distributor level	1500 [kPa]	Inner diameter	0.8 [m]
Expanded bed height	6 [m]	Butane feed	40 [Nm^3/h]
Superficial gas velocity	0.6 [m/s]	Oxygen feed	200 [Nm^3/h]
Mean particle diameter	50 [μm]	Nitrogen feed	800 [Nm^3/h]
Reactor shell preheat temperature	513 [K]		

Table 3. Kinetic parameters from Centi *et al.* (23)

Temperature [K]	k_1 [mol$^{1-\alpha}$ L$^{\alpha}$ g^{-1}s^{-1}]	k_2 [mol$^{1-\beta}$ L$^{\beta}$ g^{-1}s^{-1}]	k_3 [mol$^{\gamma-\delta}$ L$^{1-\gamma-\delta}$ g^{-1}s^{-1}]
573.15	3.357 x 10^{-7}	2.001 x 10^{-7}	4.400 x 10^{-8}
593.15	4.621 x 10^{-7}	4.364 x 10^{-7}	6.606 x 10^{-8}
613.15	6.230 x 10^{-7}	9.040 x 10^{-7}	9.658 x 10^{-8}
Other parameters:	K_B=2616 [L mol^{-1}]; $\alpha = \beta$ =0.2298 [-]; γ =0.6345 [-]; δ =1.151[-]		

Proposed Stoichiometry

The following stoichiometry is assumed for this modeling work. The CO:CO_2 molar ratio is assumed to be 1, similar to values reported by Lorences et al. (26).

R$_1$: $$C_4H_{10} + 3.5O_2 \longrightarrow C_4H_2O_3 + 4H_2O$$

R$_2$: $$C_4H_{10} + 5.5O_2 \longrightarrow 4CO_X + 5H_2O$$

R$_3$: $$C_4H_2O_3 + 2O_2 \longrightarrow 4CO_X + H_2O$$

Implementation of the general model

The general model described above is applied to a MA reactor. The dynamic model is solved by COMSOL Multiphysics 3.2b in a one-dimensional geometry as described by equations 1 to 4. Features such as gas sorption, gas chemisorption, selective membrane permeation, and intra-particle diffusion are not needed in the current computer simulations. A heat exchange term between the gas and reaction vessel is included on the left hand side of form: $+U_{(R)}\left(T_{(R)} - T_{(\varphi)}\right)$. A heat balance for the reactor vessel (made of steel) is developed in a similar way:

$$-\vec{\nabla}.\left(-\left\langle K_{(R)}\right\rangle\vec{\nabla}.\left(T_{(R)}\right)\right)+U_{(R)}a_R\left(T_{(\varphi)}-T_{(R)}\right)+U_{(Cool)}a_{cool}\left(T_{(Cool)}-T_{(R)}\right)=\frac{\partial}{\partial t}\left(\left\langle\rho_{(R)}\right\rangle\left\langle C_{P_{(R)}}\right\rangle.T_{(R)}\right) \quad \textbf{(6)}$$

where subscript "R" denotes the reactor shell. The reactor shell Biot number is low enough to ensure that the radial variation in temperature can be safely neglected, allowing for the implementation of a 1-D model. The start-up policy for solving the model requires that all species concentrations inside the reactor are equal to their input values. At t=0, all concentration profiles are flat along the reactor height. Suddenly, at t=0 the reaction and convection start, and the conversion increases gradually as time progresses. The shell is assumed to be externally preheated to 513 K, as well as insulated to prevent heat loss. Equations 1 to 4 were used to simulate the reactor, assuming an average (i.e. weighted by their fractions in the bed) temperature for the High and Low density pseudo-phases as the reactor temperature.

RESULTS AND DISCUSSION

Numerical simulation of the system dynamics unveiled two very different time scales:

Mass transfer/reaction time scale. System dynamics based on the mole balances for the chemical species inside the reactor are very quick. The time step for the numerical simulations needs to be kept below 0.0001 s to assure numerical stability due the speed of the convection-diffusion processes. The time-step required to solve the model was estimated by trial and error. The time scale in this case is ~10 s. On the other hand, heat transfer to/from the reactor vessel is very slow and has very little influence on the system dynamics for the above time scale. Conversion profiles at different times for the reactor are depicted in Figure 1. For these curves, all heat transfer processes can be assumed to be at pseudo-steady-state. The shape of the profiles is similar to earlier findings (25).

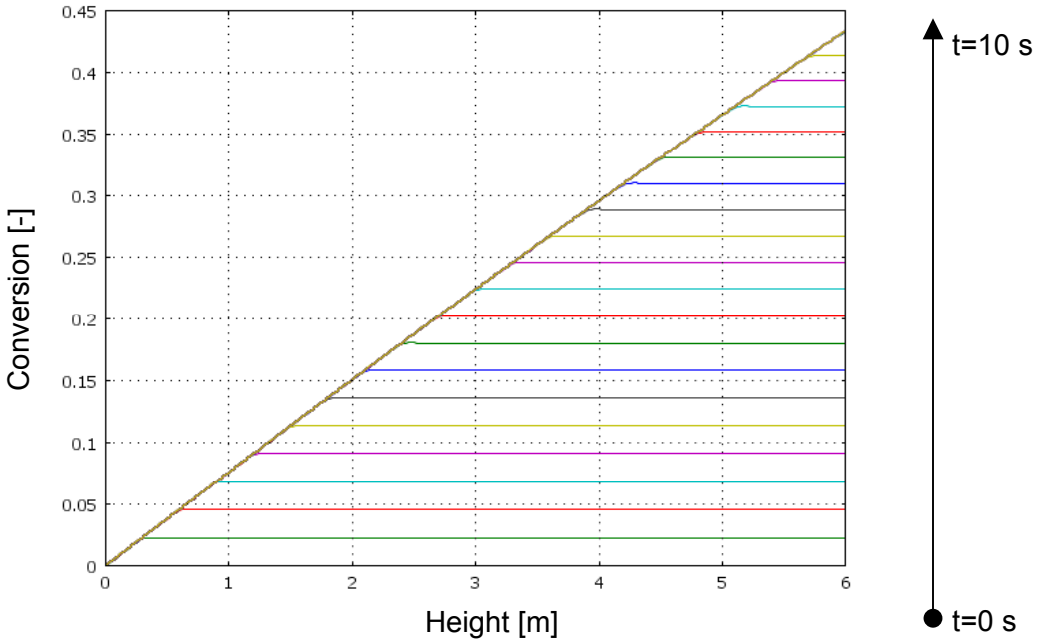

Figure 1. Conversion *vs* Height [m] for different times (one profile every 0.5 s).

Heat transfer time scale. Because of the thermal inertia of the reactor and its contents, heat transfer involves a time scale many orders of magnitude larger than the mass transfer/reaction time scale. Our simulations adopt values of the state variables and parameters from the Section 4.1 simulations after 10 s (i.e. when the mass transfer/reaction processes have essentially reached steady state). The system is then simulated by two coupled energy balances (one for the reactor contents, the other for the vessel), with species concentration profiles, rates of reaction profiles and heat generation profiles taken from Section 4.1 above. It was verified that this procedure gave overall solutions very similar to those where all of the dynamic equations were solved simultaneously.

The time step is increased to ~0.1 s, and numerical stability is conserved. 150,000 s are required to reach steady-state. This confirms that the shell temperature profile evolves, trying to equilibrate with the reactor temperature. The heat transfer is much slower than the mass transfer/reaction phenomena. Figures 2 and 3 depict temperature profiles plotted every 500 s.

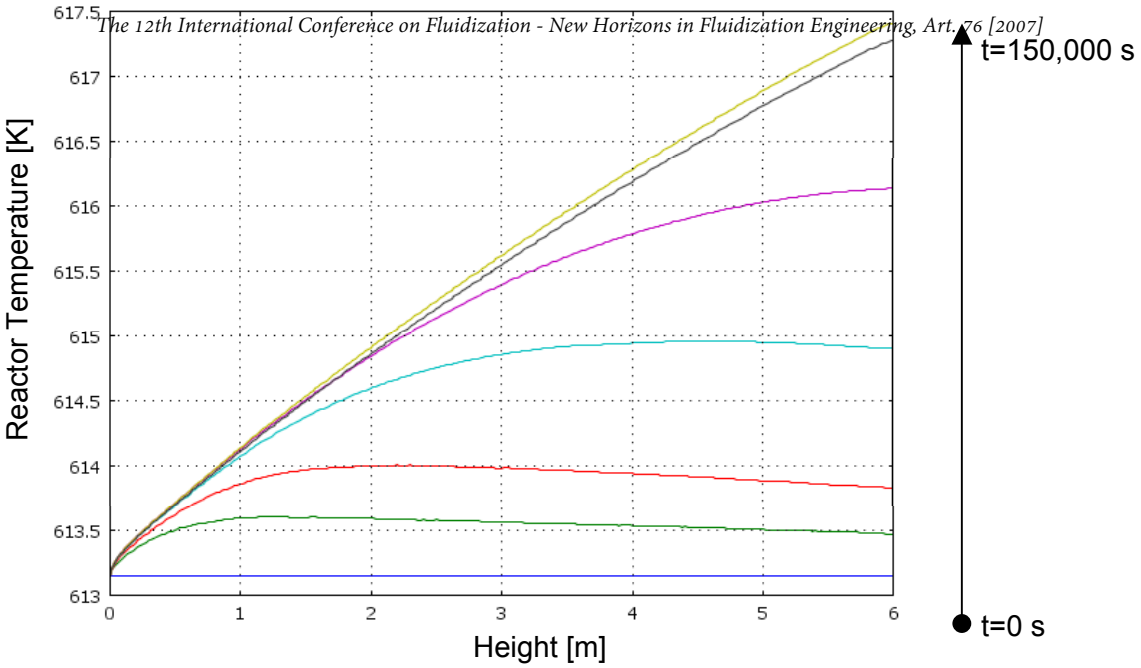

Figure 2. Reactor temperature *vs* height for different times (profiles at: t = 0 s, t = 1 s, t = 2 s, t = 5 s, t = 10 s, t = 1,000 s and t = 150,000 s).

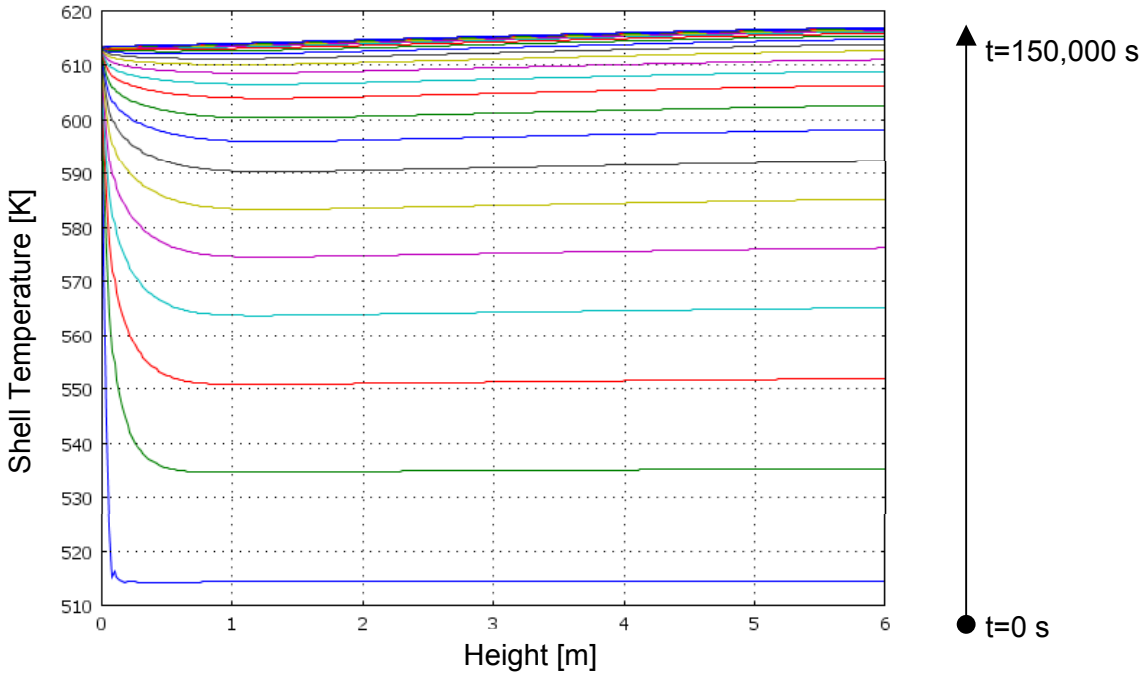

Figure 3. Reactor shell temperature *vs* height at different times. (one profile every 3,000 s).

From Figure 2 it is clear that the reactor temperature has faster dynamics than the reactor shell since it reaches almost its final value after ~1000 s. In this mode of operation it is safe to assume that the mass transfer/reaction processes are at pseudo-steady-state. The time scale for the heat transfer phenomena depend on the size of the equipment and also on whether the vessel is externally insulated or refractory-lined. Neglecting the heat effects of the reactor shell in Section 4.1 does not affect the results significantly. However, this assumption is not appropriate when estimating the time to reach thermal steady state.

CONCLUSIONS

Our general dynamic model describes fluidized bed reactors with fewer simplifying assumptions than other models in the literature. Different time scales are identified for an industrial MA reactor, providing insight into the dynamic behaviour of the system. The generalized model may be simplified depending on the desired degree of sophistication for a given period. The model predicts very different time scales for key dynamic phenomena inherent to the process. A mass transfer/reaction time scale was found to be close to the residence time of the gas molecules in the reactor. Furthermore a heat transfer time scale several orders of magnitude larger was unveiled for the current system. Heat transfer calculations may be carried out assuming that the mass transfer/reaction phenomena have reached a pseudo-steady state. In addition, it is safe to neglect heat transfer dynamics for the initial few seconds required for the mass transfer/reaction phenomena to stabilize. This type of time-scale analysis may be a useful tool to identify the appropriate degree of sophistication to predict the dynamics of complex reacting systems. Some assumptions are valid for a determined interval of time, whereas the same assumption may be invalid if applied when considering different time scales.

NOTATION

A	Area, (m^2)	N_C	Number of species in phase (φ), (dimensionless)
$C_{i_{(\varphi)}}$	Concentration of species *i* in phase (φ), (mol/m^3)	$\overrightarrow{N_{i_{(\varphi)}}}$	Vector of dispersive molar fluxes of species *i* in phase (φ), ($mol/m^2.s$)
$E_{i_{(\varphi)}}$	Internal energy of species *i* in phase (φ), (J/mol)	N_R	Number of reactions, (dimensionless)
$E_{i_{cat(\varphi)}}$	Internal energy of species *i* chemisorbed on catalyst surface in phase (φ), (J/mol)	$N_{(\varphi)}$	Number of pseudo-phases.
$E_{cat_{(\varphi)}}$	Internal energy of the catalyst in phase (φ), (J/kg)	$P_{(\varphi)}$	Pressure in phase (φ), (Pa)
$E_{i_{seq(\varphi)}}$	Internal energy of species *i* chemisorbed on solids sorbent surface in phase (φ), (J/mol)	$\overrightarrow{q_{(\varphi)}}$	Vector of dispersive molar fluxes in phase (φ), (W/m^2)
$E_{seq_{(\varphi)}}$	Internal energy of the solids sorbent in phase (φ), (J/kg)	$r_{j(\varphi)}$	Generalized rate of reaction *j* in phase (φ), (mol/kg.s)
f_C	Catalyst chemisorption function (mol/m^2)	S	Catalyst surface area per unit volume, (m^{-1})
f_S	Solid sorbent chemisorption function (mol/m^2)	t	Time, (s)
g	Gravitational acceleration, (m/s^2)	$\overrightarrow{U_{(\varphi)}}$	Vector of convective velocities of the catalyst in phase (φ), (m/s)
ΔH_j	Heat of reaction *j*, (J/mol)	*x,y,z*	Rectangular coordinates, (m)
Greek Letters			
$\alpha_{(\varphi)}$	Volume of solid sorbent per unit of total solids (sorbent + catalyst), (dimensionless)	ρ	Density, (kg/m^3)
$\varepsilon_{(\varphi)}$	Voidage of phase (φ), (dimensionless)	σ_{ij}	Stoichiometric coefficient of species *i* in reaction *j,* (dimensionless)
η_j	Effectiveness factor, (dimensionless)	χ_j	Activity coefficient (associated with catalyst deactivation), (dimensionless)
Subscripts		*gas*	Gas
cat	Catalyst	*j*	Reaction *j*
i	Compound *i*	(φ)	Phase (φ)
seq	Solid sorbent	(R)	Reactor shell (R)

REFFERENCES

1. Yates, J.G., *Fundamentals of fluidized-bed chemical processes*. 1983, London: Butterworth-Heinemann.
2. Grace, J.R., *Fluid beds as chemical reactors*, in *Gas fluidization technology*, D. Geldart, Editor. 1986, Willey, Chichester: New York.
3. Ho, T.C., *Modeling*, in *Handbook of fluidization and fluid particle systems*, W.C. Yang, Editor. 2003, Marcel Dekker Incorporated: New York.
4. Thompson, M.L., H.T. Bi, and J.R. Grace, *A generalized bubbling/turbulent fluidized bed reactor model.* Chem. Eng. Sci., 1999. **54**: p. 2175-2185.
5. Abba, I.A., J.R. Grace, and H.T. Bi, *Application of the generic fluidized-bed reactor model to the fluidized-bed membrane reactor process for steam methane reforming with oxygen input.* Ind. Eng. Chem. Res., 2003. **42**: p. 2736-2745.
6. Chen, Z., Y. Yan, and S.S.E.H. Elnashaie, *Catalyst deactivation and engineering control for steam-reforming of higher hydrocarbons in a novel membrane reformer.* Chem. Eng. Sci., 2004. **59**: p. 1965-1978.
7. Okino, M.S. and M.L. Mavrovouniotis, *Simplification of Mathematical Models of Chemical Reaction Systems.* Chemical Reviews, 1998. **98**(2): p. 391-408.
8. Muralldhar, R. and D. Ramkrlshna, *Analysis of Droplet Coalescence in Turbulent Liquid-Liquid Dispersions.* Ind. Eng. Chem. Fundam., 1986. **25**: p. 554-560.
9. Thompson, D.R. and R. Larter, *Multiple time scale analysis of two models for the peroxidase-oxidase reaction.* Chaos, 1995. **5**(2): p. 448-457.
10. Vora, N. and P. Daoutidis, *Nonlinear Model Reduction of Chemical Reaction Systems.* AIChE Journal, 2001. **47**(10): p. 2320-2332.
11. Strier, D.E. and S.P. Dawson, *Rescaling of diffusion coefficients in two-time scale chemical systems.* Journal of Chemical Physics, 2000. **112**(2): p. 825-834.
12. Mahecha-Botero, A., J.R. Grace, S.S.E.H. Elnashaie, and C.J. Lim, *Comprehensive modelling of gas fluidized-bed reactors allowing for transients, multiple flow regimes and selective removal of species.* International Journal of Chemical Reactor Engineering, 2005. **4** (A11).
13. Mahecha-Botero, A., J.R. Grace, S.S.E.H. Elnashaie, and C.J. Lim. *Comprehensive modelling of gas fluidized-bed reactors allowing for transients, multiple flow regimes and selective removal of species*. in *CRE X conference, Innovations in Chemical Reactor Engineering*. 2005. Zacatecas, Mexico.
14. Mahecha-Botero, A., J.R. Grace, S.S.E.H. Elnashaie, and C.J. Lim, *FEMLAB simulations using a comprehensive model for gas fluidized-bed reactors*, in *COMSOL Multiphysics (FEMLAB) Conference proceedings*. 2005: Boston, USA.
15. Danckwerts, P.V., *Continuous flow systems: Distribution of residence times.* Chem. Eng. Sci., 1953. **2**: p. 1-13.
16. Dente, M., S. Pierucci, E. Tronconi, M. Cecchini, and F. Ghelfi, *Selective oxidation of n-butane to maleic anhydride in fluid bed reactors: detailed kinetic investigation andreactor modelling.* Chem. Eng. Sci., 2003. **58**: p. 643-648.
17. Pugsley, T.S., G.S. Patience, F. Berruti, and J. Chaouki, *Modeling the Catalytic Oxidation of n-Butane to Maleic Anhydride in a Circulating Fluidized Bed Reactor.* Ind. Eng. Chem. Res., 1992. **31**: p. 2652-2660.
18. Golbig, K.G. and J. Werther, *Selective synthesis of maleic anhydride by spatial separation of n-butane oxidation and catalyst reoxidation.* Chem. Eng. Sci., 1997. **52**: p. 583 595.
19. Alonso, M., M.J. Lorences, M.P. Pina, and G.S. Patience, *Butane partial oxidation in an externally fluidized bed-membrane reactor.* Catalysis Today, 2001. **67**: p. 151–157.
20. Huang, X., C. Li, B. Chen, and P.L. Silveston, *Transient Kinetics of n-Butane Oxidation to Maleic Anhydride over a VPO Catalyst.* AIChE Journal, 2002. **48**: p. 846-855.
21. Wang, D. and M.A. Barteau, *Oxidation kinetics of partially reduced vanadyl pyrophosphate catalyst.* Applied Catalysis A: General, 2002. **223**: p. 205–214.
22. Contractor, R.M., *Dupont's CFB technology for maleic anhydride.* Chem. Eng. Sci., 1999. **54**: p. 5627-5632.
23. Centi, G., G. Fornasari, and F. Trifiro, *n-Butane Oxidation to Maleic Anhydride on Vanadium-Phosphorous oxides: Kinetic analysis with a tubular Flow Staked-Pelled Reactor.* Ind. Eng. Chem. Prod. Res. Dev., 1985. **24**: p. 32-37.
24. Roy, S., M.P. Dudukovic, and P.L. Mills, *A two-phase compartments model for the selective oxidation of n-butane in a circulating fluidized bed reactor.* Catalysis Today, 2000. **61**: p. 73–85.
25. Mostoufi, N., H. Cui, and J. Chaouki, *A Comparison of Two- and Single-Phase Models for Fluidized-Bed Reactors.* Ind. Eng. Chem. Res., 2001. **40**: p. 5526-5532.
26. Lorences, M.J., G.S. Patience, F.V. Diez, and J. Coca, *Butane Oxidation to Maleic Anhydride: Kinetic Modeling and Byproducts.* Ind. Eng. Chem. Res., 2003. **42**: p. 6730-6742.